Effect of Boron (Nitrogen)-Divacancy Complex Defects on the Electronic Properties of Graphene Nanoribbon

Zhiyong Wang, Junchao Jin, Mengyao Sun

College of Science, Guilin University of Technology, Guilin, China
Email: zhiyongwang520@gmail.com

Abstract

We report the effect of boron (nitrogen)-divacancy complex defects on the electronic properties of graphene nanoribbon by means of density functional theory. It is found that the defective subbands appear in the conduction band and valence band in accordance with boron (nitrogen)-divacancy defect, respectively; the impurity subbands don't lead to the transition from the metallic characteristic to a semiconducting one. These complex defects affect the electronic band structures around the Fermi level of the graphene nanoribbon; the charge densities of these configurations have also changed distinctly. It is hoped that the theoretical results are helpful in designing the electronic device.

Keywords

Complex Defects, Electronic Properties, Graphene Nanoribbon

1. Introduction

Graphene, as a (2D) monolayer honeycomb structure of carbon, has attracted a great deal of interest since its successful preparation in 2004 [1]. Due to its unique mechanical, structural and electronic properties, grapheme has been realised as an important material for numerous theoretical investigations and promising applications. Among these are charge carriers behaving as massless Dirac fermions [2], Klein tunneling [3] [4], ballistic transport at room temperature [5] [6], and anomalous quantum Hall effects [7]. From experimental points of view, field-effect transistors [8] [9], micromechanical resonators [10], gassensors of graphene have already been proposed [11]. Chemical doping aims at producing p-doped or n-doped transistors, which are crucial for building logic functions and complex circuits [12]. Doping also allows new applications such as chemical sensors or electrochemical switches [13]. In carbon-based mate-

rials p-type (n-type) doping can be achieved by boron (nitrogen) atom substitution within the carbon matrix [14]. Recently, both experimental and theoretical works have addressed the possibility to create on graphene, a single or a few number of vacancies, or even a superlattice of vacancies [15] [16] [17]. The effects of divacancy on the properties of GNRs (or Boron nitride nanoribbons) have also been investigated [18] [19] [20]. However, the effect of adatom-divacancy complex defects on the electronic properties of graphene nanoribbon (GNR) has not been investigated yet. Here we present a theoretical study of the electronic properties of GNRs with boron (nitrogen)-divacancy complex defects by means of density functional theory.

2. Calculational Method and Model

We have relaxed and calculated the electronic structures of all the considered GNRs by utilizing the SIESTA code [21] [22] [23], where the exchange-correlation potential is a generalized gradient approximation (GGA) in the form of Perdew, Burke, and Ernzerhof [24]. The atomic orbital basis set was a double-ζ plus polarization function (DZP). The numerical integrals were performed on a real space grid with an equivalent cutoff of 200 Ry. A periodic boundary condition along Y direction was applied to the GNR, while a vacuum region larger than 10 Å along the Z direction was set to decouple the interaction between adjacent GNR to ensure an isolated single-layer GNR being considered. The supercells of the perfect GNR under study contain 120 carbon atoms. The edges were terminated by hydrogens to form C–H bonds for neutralizing valencies of all the carbon atoms.

3. Results and Discussions

Firstly, we investigate the changes of geometry structures of the GNRs with boron (nitrogen)-divacancy complex defects. After the geometry relaxation, the perfect GNR is labeled as Per configuration, the GNR with only two vacancies is labeled as 2V configuration (see Figure 1(a)), the GNR with boron-divacancy complex defect is labeled as 2VB configuration (see Figure 1(b)), the GNR with nitrogen-divacancy complex defect is labeled as 2VN configuration(see Figure 1(c)), the GNR with boron-divacancy and nitrogen-divacancy, which forms the B-N bond, is labeled as 2VBN configuration (see Figure 1(d)), the GNR with boron(nitrogen)-divacancy, which forms B-B bond, is labeled as 2VBN1 configuration (see Figure 1(e)). In Figure 1(a), the divacancy structure under considered here had carbon atoms arranged and formed a geometry with two pentagonsside by side with an octagon, this configuration that we will refer from now on as a 585 divacancy. The bond lengths in the vacancyring vary between 1.390 and 1.594 Å, the longest bond is the mutual bond between pentagon and octagon, and is thus up to 13%longer than the counterpart in perfect GNR. It can be found that the bonds in the vacancy ring are strained and weaker than that in a pure sp^2 hybridization. In Figure 1(b), the bond lengths in the vacancy ring vary between 1.407 and 1.820 Å, the longest bond is the B-B bond (see Figure 1(b)), and is thus up to 29% longer than in perfect GNR, which may be attributed to the strong interaction between the two neighbouring boron atoms. In Figure 1(c), the bond lengths in the vacancy ring vary between 1.315 and 1.478 Å, the shortest bond is the N-C bond, which may be ascribed
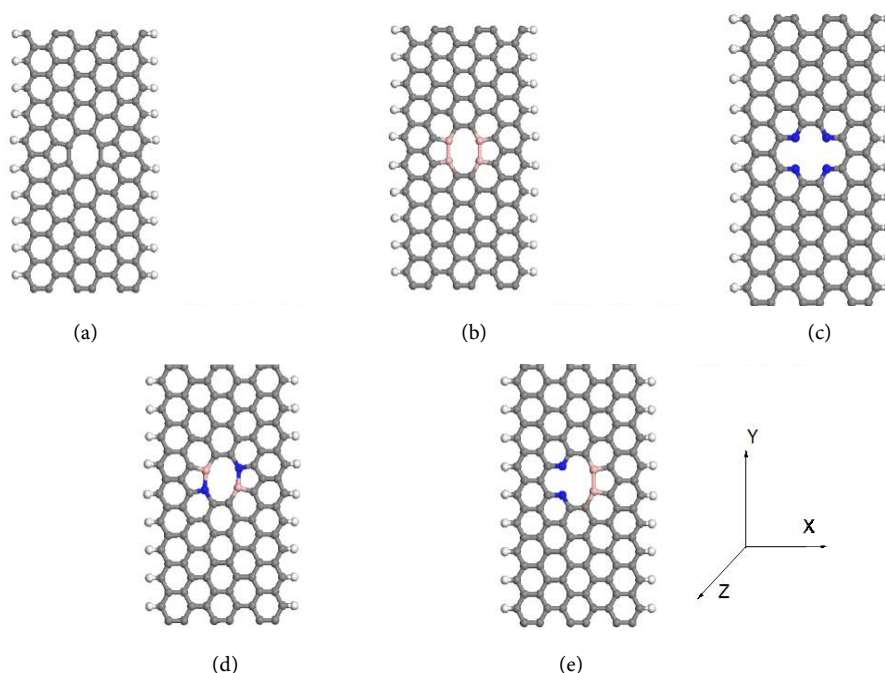
Figure 1. Fully optimized structures of five different configurations. (a) Top view of divacancy configuration, which is labeled as 2V configuration; (b) Top view of the boron-divacancy complex configuration, which is labeled as 2VB configuration; (c) Top view of the nitrogen-divacancy complex configuration, which is labeled as 2VN configuration; (d) Top view of the boron (nitrogen)-divacancy complex configuration, which is labeled as 2VBN configuration; (e) Top view of the boron (nitrogen)-divacancy complex configuration, which is labeled as 2VBN1 configuration.

to the smaller atomic radius of the nitrogen atom than that of the carbon atom, and weaker interaction between the two neighbouring nitrogen atoms, so there are four dangling bonds in the vacancy ring. In **Figure 1(d)**, the bond lengths in the vacancy ring vary between 1.387 and 1.685 Å, the longest bond is the B-N bond, which reflects the B-N bond is weaker than others bonds in the vacancy ring. In **Figure 1(e)**, the bond lengths in the vacancy ring vary between 1.331 and 1.846 Å, the longest bond is B-B bond, which is thus up to 31% longer than in perfect GNR.

The geometry structures' changes must affect the electronic band structures of these complex configurations. As shown in **Figure 2**, the electronic band structures of these configurations are investigated. In 2V configuration, the degeneracy of energy band around the Fermi level is reduced obviously compared with the Per configuration, and it appears the defect subbands near the Fermi level because of the introducing of the divacancy. In 2VB configuration, there occur new impurity subbands in the conduction band. Note that the impurity subbands do not change the metallic characteristic of the GNR, which is very different from the boron (nitrogen) substitutional doping in the perfect GNR where the impurity subbands change the metallic GNR to a semiconducting one [25]. It may be attributed to the carbon vacancy in the GNR. In 2VN configuration, there occur new impurity subbands in the valence band. It can be found that it does not change the metallic characteristic of the GNR, pyridinic nitrogen atom forms two covalent bonds with each nearest neighboring carbon atom and contributes one p electron to the π electron systems of the GNR. The impurity next to the carbon vacancy
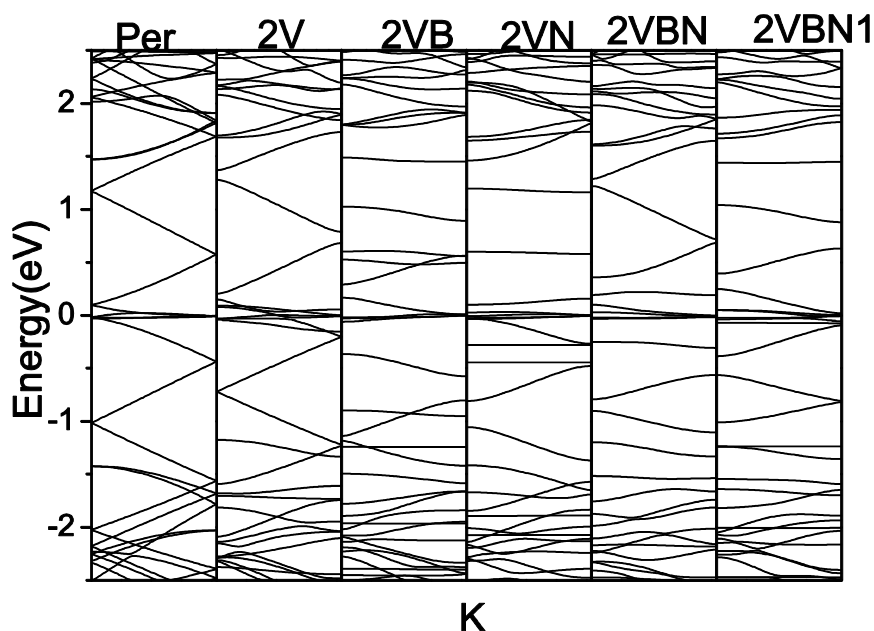
Figure 2. The electronic band structures of the GNRs with boron (nitrogen)-divacancy complex defects. The Fermi level is set at 0 eV. The wave vector is from Γ to X.

is strongly electronegative because of the neighboring vacancy and the p electron is localized around the nitrogen atom. In 2VBN and 2VBN1 configurations, the degeneracy of energy band around the Fermi level is reduced distinctly compared with the Per configuration, the lowest unoccupied band and the highest occupied band of the 2VBN1 are more closing to the Fermi level compared with the 2VBN configuration, it may be attributed to the presence of pyridinic nitrogen atom.

Next we will continue to investigate the effect of boron (nitrogen)-divacancy complex defect on the charge density of the GNR. In **Figure 3(a)**, the charge densities in the region of two pentagons increase compared with the counterpart of the Per configuration, and the charge densities of the centre region of the octagon are nearly zero. It may be attributed to the charge transfer from the carbon atom of the octagon to the carbon atom of two pentagons. In **Figure 3(b)**, the charge densities of four boron atoms decrease compared with the counterpart of the 2V configuration, which may be ascribed to the strong interaction between two neighbouring boron atoms. In **Figure 3(c)**, the charge densities near four nitrogen atoms increase compared with the counterpart of the 2VB configuration, because of the neighbouring vacancy and the p electron is localized in the round of nitrogen, and the charge densities of the centre region of the vacancy ring have also changed. In **Figure 3(d)**, the charge densities of the vacancy ring have changed distinctly because of the formation B-N bond, the charge densities around the nitrogen atom are higher than that of the boron atom, which may be attributed to the charge transfer from the boron atom to the neighbouring nitrogen atom. In **Figure 3(e)**, the charge densities around the neighbouring carbon atom of the nitrogen atom are higher than the counterpart of the 2VN configuration because of the coupling between the boron atom and nitrogen atom, and the zero charge density of the centre region of the vacancy ring is smaller than that of the 2VBN configuration.
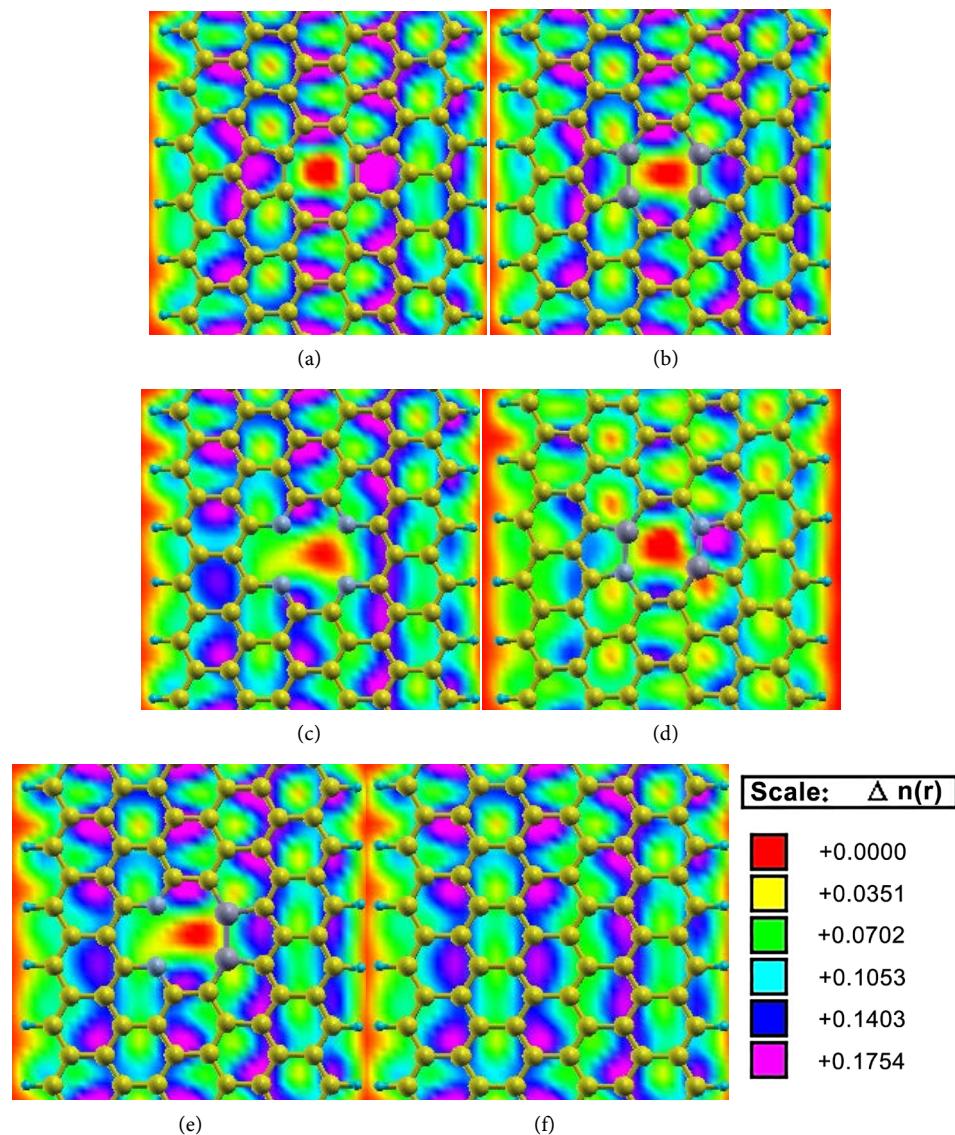
Figure 3. The charge densities around the defect are plotted, (a) (b) (c) (d) and (e) refer to the 2V, 2VB, 2VN, 2VBN and 2VBN1 configurations, respectively. (f) refers to the charge density of the Per configuration for comparison.

4. Conclusion

In this paper, we have investigated the effects of boron nitrogen)-divacancy complex defects on the electronic properties of the GNR. Firstly, we have analyzed the geometry structures of these complex configurations; it is found that boron-divacancy complex defect can form the B-B or B-N bonds with the neighbouring boron atom or nitrogen atom, while for the nitrogen-divacancy complex configuration, which forms four dangling bonds. Secondly, we have investigated the electronic band structures of these complex defects; the calculated results show that the boron(nitrogen)-divacancy complex configurations do not change the metallic characteristic; the coupling between the defect state and impurity state only affects the conduction band and valence band around the Fermi level, respectively. Lastly, we have also investigated the charge densities of these complex configurations; it is very different between the nitrogen-divacancy

and boron-divacancy. It is hoped that the theoretical discussions may be helpful in investigating the transport property and designing the electronic device.

Acknowledgements

References

[1] Novoselov, K.S., Geim, A.K., Morozov, S.V., Jiang, D., Zhang, Y., Dubonos, S.V., Grigorieva, I.V. and Firsov, A.A. (2004) Electric Field Effect in Atomically Thin Carbon Films. *Science*, **306**, 666-669. https://doi.org/10.1126/science.1102896

[2] Novoselov, K.S., Geim, A.K., Morozov, S.V., Jiang, D., Katsnelson, M.I., Grigorieva, I.V., Dubonos, S.V. and Firsov, A.A. (2005) Two-Dimensional Gas of Massless Dirac Fermions in Graphene. *Nature*, **438**, 197-200. https://doi.org/10.1038/nature04233

[3] Katsnelson, M.I., Novoselov, K.S. and Geim, A.K. (2006) Chiraltunnelling and the Klein paradox in Graphene. *Nature Physics*, **2**, 620-625. https://doi.org/10.1038/nphys384

[4] Young, A.F. and Kim, P. (2009) Quantum Transport and Klein Tunneling in Graphene Heterojunctions. *Nature Physics*, **5**, 222-226. https://doi.org/10.1038/nphys1198

[5] Gunlycke, D., Lawler, H.M. and White, C.T. (2007) Room-Temperature Ballistic Transport in Narrow Graphene Strips. *Physical Review B*, **75**, Article ID: 085418. https://doi.org/10.1103/physrevb.75.085418

[6] Du, X., Skachko, I., Barker, A. and Andrei, E.Y. (2008) Approaching Ballistic Transport in Suspended Graphene. *Nature Nanotechnology*, **3,** 491-495. https://doi.org/10.1038/nnano.2008.199

[7] Novoselov, K.S., Jiang, Z., Zhang, Y., Morozov, S.V., Stormer, H.L., Zeitler, U., Maan, J.C., Boebinger, G.S., Kim, P. and Geim, A.K. (2007) Room-Temperature Quantum Hall Effect in Graphene. *Science*, **315**, 1379. https://doi.org/10.1126/science.1137201

[8] Wang, X., Ouyang, Y., Li, X., Wang, H., Guo, J. and Dai, H. (2008) Room-Temperature All-Semiconducting Sub-10-nm Graphene Nanoribbon Field-Effect Transistors. *Physical Review Letters*, **100**, Article ID: 206803. https://doi.org/10.1103/physrevlett.100.206803

[9] Lin, Y.-M., Dimitrakopoulos, C., Jenkins, K.A., Farmer, D.B., Chiu, H.-Y., Grill, A. and Avouris, Ph. (2010) 100-GHz Transistors from Wafer-Scale Epitaxial Graphene. *Science*, **327**, 662. https://doi.org/10.1126/science.1184289

[10] Sidorenko, A., Krupenkin, T., Taylor, A., Fratzl, P. and Aizenberg, J. (2007) Reversible Switching of Hydrogel-Actuated Nanostructures into Complex Micropatterns. *Science*, **315**, 487-490. https://doi.org/10.1126/science.1135516

[11] Schedin, F., Geim, A.K., Morozov, S.V., Hill, E.W., Blake, P., Katsnelson, M.I. and Novoselov, K.S. (2007) Detection of Individual Gas Molecules Adsorbed on Graphene. *Nature Materials*, **6**, 652-655. https://doi.org/10.1038/nmat1967

[12] Derycke, V., Martel, R., Appenzeller, J. and Avouris, P. (2001) Carbon Nanotube Inter-and Intramolecular Logic Gates. *Nano Letters*, **1**, 453-456. https://doi.org/10.1021/nl015606f

[13] Wehling, T.O., *et al*. (2008) Molecular Doping of Graphene. *Nano Letters*, **8**, 173-177. https://doi.org/10.1021/nl072364w

[14] Terrones, M., *et al*. (1996) Pyrolytically Grown $B_xC_yN_z$ Nanomaterials: Nanofibres and Nanotubes. *Chemical Physics Letters*, **257**, 576-582. https://doi.org/10.1016/0009-2614(96)00594-5

[15] Pedersen, T.G., Flindt, C., Pedersen, J., Mortensen, N.A., Jauho, A.P. and Pedersen, K. (2008) Graphene Antidot Lattices: Designed Defects and Spin Qubits. *Physical Review Let-*

ters, **100**, Article ID: 136804. https://doi.org/10.1103/physrevlett.100.136804

[16] Rosales, L., Pacheco, M., Barticevic, Z., León, A., Latgé, A. and Orellana, P.A. (2009) Transport Properties of Antidotsuperlattices of Graphene Nanoribbons. *Physical Review B*, **80**, Article ID: 073402. https://doi.org/10.1103/PhysRevB.80.073402

[17] Carlsson, J.M. and Scheffler, M. (2006) Structural, Electronic, and Chemical Properties of Nanoporous Carbon. *Physical Review Letters*, **96**, Article ID: 046806. https://doi.org/10.1103/physrevlett.96.046806

[18] Jaskólski, W., Chico, L. and Ayuela, A. (2015) Divacancy-Induced Ferromagnetism in Graphene Nanoribbons. *Physical Review B*, **91**, Article ID: 165427. https://doi.org/10.1103/physrevb.91.165427

[19] Zhang, H., Yu, G., Chen, W., Guan, J. and Huang, X. (2015) A First-Principles Investigation on the Effect of the Divacancy Defect on the Band Structures of Boron Nitride (BN) Nanoribbons. *Physica E*, **69**, 65-74. https://doi.org/10.1016/j.physe.2015.01.024

[20] Chakrabarty, S., Abdul Wasey, A.H.M., Thapa, R. and Das, G.P. (2015) First Principles Design of Divacancy Defected Graphene Nanoribbon Based Rectifying and Negative Differential Resistance Device. *AIP Advances*, **5**, Article ID: 087163. https://doi.org/10.1063/1.4929576

[21] Ordejón, P., Artacho, E. and Soler, J.M. (1996) Self-Consistent Order-N Density-Functional Calculations for Very Large Systems. *Physical Review B*, **53**, R10441-R10444. https://doi.org/10.1103/PhysRevB.53.R10441

[22] Sánchez-Portal, D., Ordejón, P., Artacho, E. and Soler, J.M. (1997) Density-Functional Method for Very Large Systems with LCAO Basis Sets. *International Journal of Quantum Chemistry*, **65**, 453-461. https://doi.org/10.1002/(SICI)1097-461X(1997)65:5<453::AID-QUA9>3.0.CO;2-V

[23] Soler, J.M., Artacho, E., Gale, J.D., García, A., Junquera, J., Ordejón, P. and Sánchez-Portal, D. (2002) The SIESTA Method for *ab Initio* Order-N Materials Simulation. *Journal of Physics: Condensed Matter*, **14**, 2745-2779. https://doi.org/10.1088/0953-8984/14/11/302

[24] Perdew, J.P., Burke, K. and Ernzerhof, M. (1996) Generalized Gradient Approximation Made Simple. *Physical Review Letters*, **77**, 3865-3868. https://doi.org/10.1103/PhysRevLett.77.3865

[25] Huang, B., Yan, Q., Zhou, G., Wu, J., Gu, B., Duan, W. and Liu, F. (2007) Making a Field Effect Transistor on a single Graphene Nanoribbon by Selective Doping. *Applied Physics Letters*, **91**, Article ID: 253122. https://doi.org/10.1063/1.2826547